Increased Ca^{2+} influx through Na$^+$/Ca^{2+} exchanger during long-term facilitation at crayfish neuromuscular junctions

Akira Minami, Yan-fang Xia and Robert S. Zucker

Department of Molecular and Cell Biology and Helen Wills Neuroscience Institute, University of California, Berkeley, CA 94720, USA

Intense motor neuron activity induces a long-term facilitation (LTF) of synaptic transmission at crayfish neuromuscular junctions (NMJs) that is accompanied by an increase in the accumulation of presynaptic Ca^{2+} ions during a test train of action potentials. It is natural to assume that the increased Ca^{2+} influx during action potentials is directly responsible for the increased transmitter release in LTF, especially as the magnitudes of LTF and increased Ca^{2+} influx are positively correlated. However, our results indicate that the elevated Ca^{2+} entry occurs through the reverse mode operation of presynaptic Na$^+$/Ca^{2+} exchangers that are activated by an LTF-inducing tetanus. Inhibition of Na$^+$/Ca^{2+} exchange blocks this additional Ca^{2+} influx without affecting LTF, showing that LTF is not a consequence of the regulation of these transporters and is not directly related to the increase in [Ca^{2+}]$_i$ reached during a train of action potentials. Their correlation is probably due to both being induced independently by the strong [Ca^{2+}]$_i$ elevation accompanying LTF-inducing stimuli. Our results reveal a new form of regulation of neuronal Na$^+$/Ca^{2+} exchange that does not directly alter the strength of synaptic transmission.

Crustacean neuromuscular junctions display numerous forms of synaptic plasticity in which transmission is strengthened following previous activity. Long-term facilitation is one such form of synaptic enhancement that is prominent at crayfish tonic limb NMJs, whereby extensive motor neuron activity results in increased release of transmitter evoked by subsequent action potentials by activating previously 'silent' synapses (Wojtowicz & Atwood, 1985, 1986, 1988; Wojtowicz *et al.* 1988, 1994). LTF results from an accumulation of Na$^+$ ions during intense presynaptic activity, whose extrusion by an electrogenic Na$^+$/K$^+$ pump results in a post-tetanic hyperpolarization that activates presynaptic hyper-polarization and cyclic nucleotide-activated (HCN) channels; these act in concert with the actin cytoskeleton and [Ca^{2+}]$_i$ elevated by conditioning activity through a calcineurin-sensitive kinase cascade to synthesize proteins that awaken synapses (Beaumont *et al.* 2001, 2002; Zhong & Zucker, 2004).

Glutamatergic crustacean and insect NMJs are also regulated by circulating hormones such as serotonin, which can strongly increase the number of transmitter quanta released (or the number of synaptic vesicles that fuse) to an action potential (Dudel, 1965; Glusman & Kravitz, 1982; Fischer & Florey, 1983; Yoshihara *et al.* 1999, 2000; Kuromi & Kidokoro, 2000). At crayfish

and *Drosophila* NMJs, presynaptic serotonin receptors coupled to adenylyl cyclase produce cAMP to enhance transmission by activation of two pathways – one involving the same HCN channels that are involved in LTF induction and another involving exchange protein activated by cAMP (EPAC) (Beaumont & Zucker, 2000; Zhong & Zucker, 2005; Cheung *et al.* 2006). In this case synaptic enhancement is short-lived, presumably because the Ca^{2+}-dependent activation of protein synthesis and a phosphatase/kinase cascade are absent (Beaumont *et al.* 2001).

The HCN-dependent enhancement of transmission by serotonin is mediated by the recruitment of a dormant or non-recycling vesicle pool, rather than by an increase in the probability of release of vesicles from a previously available pool (Wang & Zucker, 1998; Lin & Fu, 2005), and our preliminary observations (V. Beaumont and R. Zucker, unpublished) suggest that LTF is similarly expressed, involving increased vesicle availability and synapse activation.

In an effort to understand how HCN channel activation might regulate synaptic transmission, we found that presynaptic Ca^{2+} ions entering through HCN channels could not account for LTF (Zhong *et al.* 2004). In the course of these experiments, we observed that the presynaptic [Ca^{2+}]$_i$ rise in a burst of action potentials increased

following LTF induction. Our initial interpretation (Xia & Zucker, 2005) was that LTF was caused by increased Ca^{2+} influx through the voltage-dependent Ca^{2+} channels that trigger neurosecretion. Subsequent investigation has caused us to revise this interpretation. Here we present evidence that increased Ca^{2+} accumulation in bursts following LTF-inducing stimuli is due to a stimulation of Ca^{2+} influx through up-regulated Na^+/Ca^{2+} exchangers. We also show that this increased Ca^{2+} influx is unrelated to LTF expression.

Methods

Preparation

Crayfish (*Procambarus clarkii*; 5.0–7.0 cm) were obtained from Atchafalaya Biological Supply (Raceland, LA, USA) or Niles Biological (Sacramento, CA) and treated in accordance with institutional guidelines. Preparation of the innervated dactyl opener muscle of the first walking leg has previously been described (Delaney *et al.* 1991; Landò & Zucker, 1994). First walking legs were removed by natural autotomy and immersed in ice-cold low-Ca^{2+}, high-Mg^{2+} modified Van Barneveld's (MVH) solution containing (mM): NaCl 195, KCl 5.4, $CaCl_2$ 2.5, $MgCl_2$ 13.5, and Na-Hepes 10 (pH 7.4). This solution suppresses synaptic transmission and prevents the spurious induction of LTF. Legs were pinned on a Sylgard-lined chamber, covered with 4 ml of ice cold MVH solution. The ventral surface of the opener muscle was exposed by removal of the shell and closer muscle while the leg nerve was dissected from the meropodite. The preparation was continuously perfused at 2 ml min^{-1} with normal Van Harreveld's solution at 15–17°C, containing (mM): NaCl 195, KCl 5.4, $CaCl_2$ 13.5, $MgCl_2$ 2.6 and Na-Hepes 10 (pH 7.4). In calcium free solution, $MgCl_2$ replaced the $CaCl_2$. 2-[2-[4-(4-Nitrobenzyloxy)phenyl]ethyl]isothiourea (KB R7943) was obtained from Nippon Organon (Tokyo, Japan). The following products were purchased from the vendors indicated: fura-2 and fluo-4 pentapotassium salts (Invitrogen, Eugene, OR, USA); Sodium-binding benzofuran isophthalate (SBFI) (TefLabs, Austin, TX); palytoxin (Wako Industries, Tokyo, Japan); Gramicidin A (Sigma-Aldrich, St Louis, MO, USA); and monensin (Calbiochem, San Diego, CA, USA). Stock solutions of KB R7943 (100 mM) were made in dimethyl sulfoxide (DMSO) and diluted to 20 μM in crayfish Ringer solution before experiments; the final concentration of DMSO was 0.02%.

Electrophysiology

The exciter motor axon to the opener muscle was selectively stimulated at 1 Hz by suction electrode in the meropodite (test responses), or at 10 Hz for 1 min (brief tetanus, BT) or 20 Hz for 10 min (LTF-inducing tetanus, LTFIT). Excitatory junctional potentials (EJPs) were recorded by impaling a proximal muscle fibre with a microelectrode (10–30 MΩ, filled with 3 M KCl). In some experiments, presynaptic potentials were recorded by impaling a primary branch of the exciter axon with a sharp microelectrode (50–80 MΩ, filled with 3 M KCl). Electrical signals were amplified and filtered at 2 kHz (Neuroprobe 1600, A-M Systems, Everett, WA, USA) and digitized at 5 kHz (DigiData 1320A, Axon Instruments, Union City, CA, USA). EJPs and action potentials were collected and analysed on-line using pCLAMP9 software (Axon Instruments); EJP amplitudes were measured from foot to peak.

$[Ca^{2+}]_i$ measurement

The exciter axon was penetrated with a bevelled electrode (50–80 MΩ) filled with fura-2 (17 mM in 200 mM KCl). Fura-2 was iontophoresed into the axon using 15 nA of continuous hyperpolarizing current for 10–15 min. Fura-2 was excited at 350 nm, and fluorescence emission above 535 nm was monitored in the presynaptic boutons during the injection. The final fura-2 concentration in boutons was estimated as 50–100 μM by comparing the fluorescence of 50 μM fura-2 solution in a microcuvette of 20 μm path-length with the intensity in presynaptic branches having a diameter of 5–10 μm. After fura-2 injection, the injection electrode was replaced with one filled with 3 M KCl. Fura-2 was alternately excited at 350 and 385 nm with a T.I.L.L. Photonics Polychrome II spectrophotometer (Eugene, OR, USA). Fluorescence was measured with a CCD camera (Sensicam, Cooke, Auburn Hills, MI, USA), through a UV-transmitting 40× water immersion objective (NA 0.7, Olympus, Tokyo, Japan), a 400 nm dichroic mirror and a 535 nm barrier filter (Chroma Technology, Rockingham, VT, USA). Regions of interest (about 5 μm diameter) were set in synaptic boutons on the same muscle fibre that was used for EJP recording. Background fluorescence from the muscle surface before fura-2 injection was subtracted from all images, and a shading correction was performed, based on a uniform field of fura-2 fluorescence from a microcuvette, using Imaging Workbench 5.2 (Indec Biosystems, Santa Clara, CA, USA) software. Shading correction corrects for both non-uniformity of illumination and colour changes due to filter and lamp ageing. Ratiometric images were acquired once per second.

Fura-2 calibration

$[Ca^{2+}]_i$ was estimated from the ratio of fura-2 emission when excited at 385 nm to emission when excited at 350 nm. Fluorescence signals were calibrated by fitting a calibration curve of fluorescence ratio *versus* $[Ca^{2+}]$

measured from microcuvettes containing 50 μM of fura-2 in solutions resembling crayfish cytoplasm (280 mM ionic strength, pH 7.02) buffered to different [Ca^{2+}] levels: (1) zero-calcium (concentrations in mM): NaCl 17, potassium D-gluconate 193, Mops 20, K$_2$EGTA 20; (2) 162 nM calcium: NaCl 17, potassium D-gluconate 208, Mops 20, K$_2$EGTA 15, CaEGTA 5; (3) 500 nM calcium: NaCl 17, potassium D-gluconate 223, Mops 20, K$_2$EGTA 10, CaEGTA 10; (4) 1.45 μM calcium: NaCl 17, potassium D-gluconate 238, Mops 20, K$_2$EGTA 5, CaEGTA 15; or (5) 25 μM calcium: NaCl 17, potassium D-gluconate 213, Mops 20, K$_3$HDPTA 8, K$_2$CaDPTA 2, where DPTA stands for 1, 3-diaminopropane-2-ol-N-N'-tetraacetic acid. A calibration curve based on eqn (5) of Grynkiewicz *et al.* (1985) was fitted to a plot of fluorescence ratios *versus* [Ca^{2+}], yielding the following parameters: $K_D = 225$ nM, $R_{max} = 7.28$, $R_{min} = 0.75$ and $S_f/S_b = 8.79$. Ratios measured in terminals were converted to [Ca^{2+}]$_i$ after application of a viscosity correction corresponding to a 30% reduction in minimum and maximum 350 nm/385 nm fluorescence ratios (Mulkey & Zucker, 1992).

Simultaneous measurement of [Ca^{2+}]$_i$ and [Na$^+$]$_i$

The exciter axon was penetrated with a bevelled electrode (14 MΩ) filled with 25 mM fluo-4 and 40 mM SBFI in a carrier solution (200 mM KCl and 10 mM K-Hepes, pH 8.5). Pressure injection used trains of eight pressure pulses (40 psi, 500 ms duration, 0.2 Hz). To estimate dye concentrations in boutons, we measured the fluorescence of a solution containing 250 μM fluo-4 and 400 μM SBFI in a microcuvette, excited by 378 nm (isosbestic point of SBFI, no fluo-4 excitation at low [Ca^{2+}]$_i$) and compared with the intensity in presynaptic boutons. Final concentrations of fluo-4 and SBFI in the bouton were about 280 μM and 450 μM, respectively. The two dyes were alternately excited at 470 nm for fluo-4, and 350 and 385 nm for SBFI. Fluorescence was measured using a 505 nm dichroic mirror (Chroma) and a 545 $\pm$ 38 nm bandpass filter (Omega Optical, Brattleboto, VT, USA).

Fluo-4 calibration

[Ca^{2+}]$_i$ was estimated from fluo-4 emission excited at 470 nm (no SBFI excitation). Fluo-4 signals were calibrated by measuring the fluorescence intensity from microcuvettes containing 250 μM fluo-4 and 400 μM SBFI in solutions (280 mM ionic strength, pH 7.02) buffered to different [Ca^{2+}] levels: (1) zero-calcium: NaCl 17, potassium D-gluconate 193, Mops 20, K$_2$EGTA 20; (2) 200 nM calcium: NaCl 17, potassium D-gluconate 211, Mops 20, K$_2$EGTA 14.2, CaEGTA 5.8; (3) 600 nM calcium: NaCl 17, potassium D-gluconate 226, Mops 20, K$_2$EGTA 8.9, CaEGTA 11.1; (4) 2 μM calcium:

NaCl 17, potassium D-gluconate 241, Mops 20, K$_2$EGTA 3.9, CaEGTA 16.1; or (5) 364 μM calcium: NaCl 17, potassium D-gluconate 216, Mops 20, K$_3$HDPTA 2.5, K$_2$CaDPTA 7.5. Plotting fluorescence intensity *versus* [Ca^{2+}] yielded a calibration curve with the following parameters: $K_D = 2.2$ mM, $F_{max} = 523$, $F_{min} = 5.1$. For experimental [Ca^{2+}]$_i$ measurements, F_{max} and F_{min} need to be adjusted for the fluo-4 concentration, bouton thickness, and effects of light scattering through underlying muscle, which are difficult to estimate accurately. By assuming that the resting fluorescence corresponds to a resting [Ca^{2+}]$_i$ of 93 nM, equal to the average resting [Ca^{2+}]$_i$ in all experiments using fura-2, we could correct for the effects of dye concentration and path length and produce a calibration curve for each experiment, as described in Lau *et al.* (1999).

SBFI calibration

SBFI was calibrated *in situ* (Harootunian *et al.* 1989) by using the sodium ionophores palytoxin, gramicidin A, and monensin. Since palytoxin inhibits the Na$^+$/K$^+$-ATPase (Habermann, 1989), [Na$^+$]$_i$ can reach a high level when external [Na$^+$] is elevated. Ratiometric fluorescence images of SBFI were measured in terminals after perfusion with varying [Na$^+$] solutions (0–257 mM Na$^+$, 280 mM ionic strength, pH 7.02), which was made by mixing a 'high Na$^+$' solution containing (mM) NaCl 13, sodium gluconate 244, Cs-Hepes 10, CaCl$_2$ 5, and MgCl$_2$, with a 'Na-free' solution, in which Na$^+$ was replaced with K$^+$. The Na$^+$-SBFI calibration parameters were $K_D = 22.8$ mM, $R_{max} = 6.02$, $R_{min} = 3.19$ and $S_f/S_b = 4.59$.

Statistical analysis

Student's paired *t* test or Fischer's sign test was used for comparison of the means of paired data. For multiple comparisons, ANOVA followed by Bonferroni's multiple comparison test was performed.

Results

The Ca^{2+} influx during action potentials increases after LTF induction

The initial discovery that motivated this study is illustrated in Fig. 1. To establish the amplitude of baseline transmission, the exciter motor neuron to the leg opener muscle was stimulated at 1 Hz while recording EJPs from the muscle and [Ca^{2+}]$_i$ changes in a presynaptic bouton transmitting to the same muscle fibre. Presynaptic [Ca^{2+}]$_i$ transients evoked by single action potentials are too small to be detected by a camera without extensive averaging (Tang *et al.* 2000). This steady low frequency stimulation was interrupted every 10 min by a 1 min brief tetanus (BT), consisting of a burst of action potentials

at 10 Hz. Synaptic facilitation and augmentation result in EJPs in these bursts that are much larger, up to 7 times those at 1 Hz, and accumulation of residual Ca^{2+} entering during the action potentials of such bursts is also substantial (Delaney & Tank, 1994), reaching 100 nM above the resting $[Ca^{2+}]_i$ in this preparation. After 40 min of this pattern of stimulation, a more intense and prolonged tetanus (20 Hz for 10 min) was generated in the motor neuron, producing an even greater increase in synaptic transmission by recruiting synaptic potentiation, which is accompanied by a larger increase in the accumulation of presynaptic Ca^{2+}.

Stimulation at 1 Hz was resumed after this strong tetanus. Facilitation and augmentation dissipated rapidly (within about 1 s and 7 s, respectively), and the third

phase of activity-dependent enhancement of synaptic transmission (potentiation, or post-tetanic potentiation (PTP) as it is traditionally called) was still dropping 1 min later, when the pattern of brief 1 min 10 Hz tetani repeated every 10 min was reinstated. This burst generated EJPs displaying both facilitation and augmentation growing during the burst, plus some potentiation from the strong tetanus that had not yet decayed. The residual Ca^{2+} underlying PTP is still decaying at this time (Delaney & Tank, 1994; Kamiya & Zucker, 1994), so that it is difficult to be certain, but it appears that the increment in $[Ca^{2+}]_i$ during this burst is larger than it was before the strong tetanus.

By the time of subsequent brief tetani, EJP augmentation and PTP as well as the corresponding phases of residual
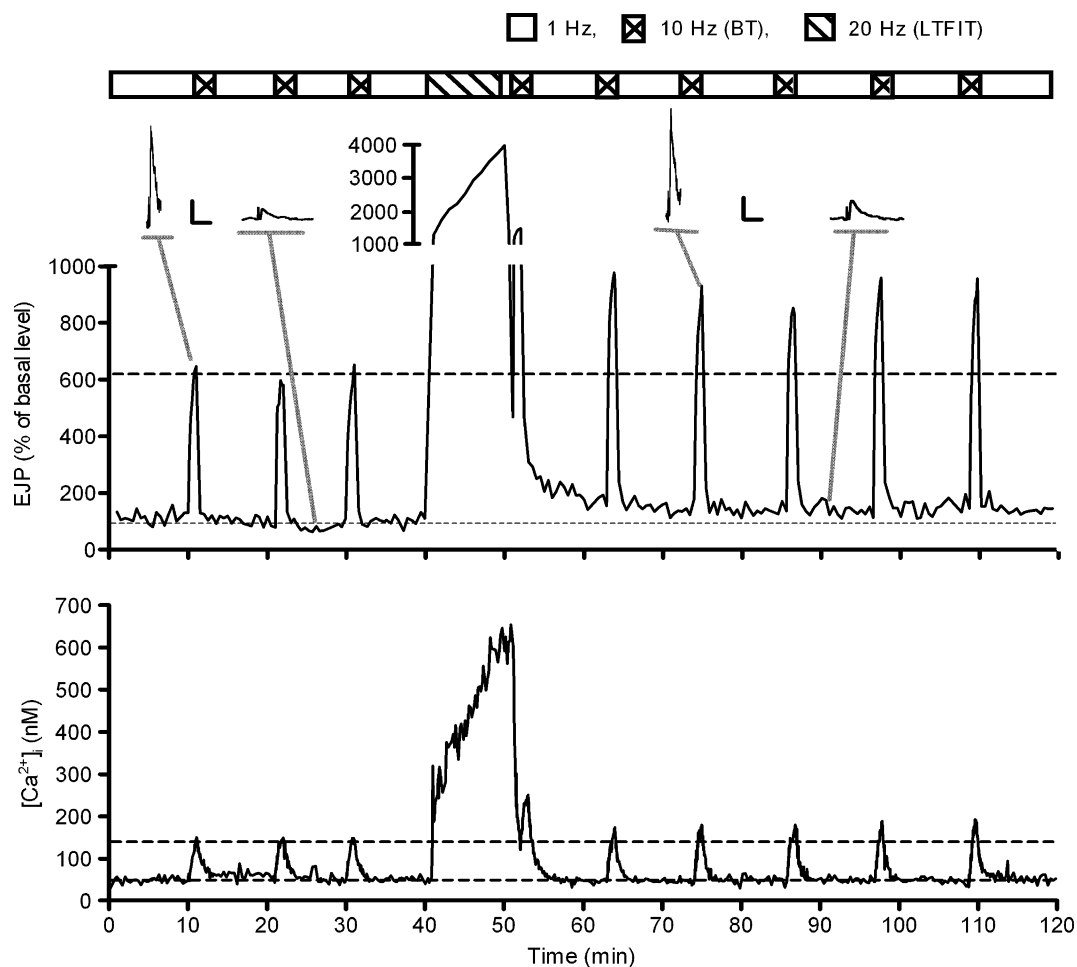
Figure 1. EJPs and presynaptic $[Ca^{2+}]_i$ transients are increased by an LTF-inducing tetanus (LTFIT)
The upper graph plots amplitudes of successive EJPs in the crayfish leg opener muscle (normalized to the initial amplitude) evoked by stimulating the motor neuron at 1 Hz, with brief tetani (BT, 10 Hz for 1 min), and with an LTF-inducing tetanus (20 Hz for 10 min). Insets show sample recordings corresponding to the responses indicated, with calibration bars of 1 mV and 50 ms. The lower graph plots presynaptic $[Ca^{2+}]_i$ calculated from fura-2 ratiometric fluorescence measurements in a presynaptic bouton imaged on the muscle fibre whose EJPs were simultaneously recorded. LTF is expressed as an increase in 1 Hz and 10 Hz EJPs following the LTF-inducing tetanus, and is accompanied by an increase in $[Ca^{2+}]_i$ transients, suggesting that increased presynaptic Ca^{2+} influx underlies LTF.

Ca^{2+} had all dissipated. What remains is the very long lasting facilitation of baseline or 1 Hz transmission called LTF, which is not caused or accompanied by any residual Ca^{2+} remaining from the strong tetanus. The strong tetanus is therefore termed an LTF-inducing tetanus. Now it is clear that the rise in [Ca^{2+}]$_i$ accompanying the next brief tetanus is substantially larger than before the LTF-inducing tetanus, and transmission during this burst remains elevated just as does baseline transmission, both manifestations of LTF. This is true of subsequent bursts of action potentials, repeated for an hour or longer after the LTF-inducing tetanus.

We felt that the most straightforward interpretation of this result was as follows: following an LTF-inducing tetanus, there is an increase in the rise in [Ca^{2+}]$_i$ during a brief train, and this is likely to reflect an increased influx in Ca^{2+} ions through the P-type Ca^{2+} channels opened by action potentials and supporting transmitter release (Wright *et al.* 1996; Allana & Lin, 2004). This, then, explains immediately why the EJPs in such bursts are larger. Presumably, the undetectable Ca^{2+} influx to single action potentials is similarly increased after the LTF-inducing tetanus, and this produces the persistent increase in baseline transmission at 1 Hz. Thus, LTF is the expression of the effects of an increase in Ca^{2+} influx during action potentials. Since the action potential waveform is unchanged during LTF (Wojtowicz & Atwood, 1985; Beaumont *et al.* 2002), the results would suggest that LTF is the result of an up-regulation of presynaptic P-type Ca^{2+} channels. Previous discussions of possible LTF expression mechanisms (Atwood & Wojtowicz, 1986; Wojtowicz *et al.* 1994; Beaumont *et al.* 2001) have favoured a modulation of the transmitter release apparatus. However, a careful review of the literature revealed little evidence in favour of, or against, a major role for Ca^{2+} channel modulation. We therefore attempted to determine the relationship between this increase in presynaptic [Ca^{2+}]$_i$ during brief bursts and LTF expression.

### LTF magnitude is weakly correlated with the increase in [Ca^{2+}]$_i$ in a brief tetanus

If the increase in [Ca^{2+}]$_i$ transients were causally related to LTF as in the above hypothesis, then the two should be closely correlated. Figure 2 plots the results of 23 experiments like that illustrated in Fig. 1, showing a weak but significant correlation ($r = 0.53$, $P = 0.0094$). The correlation becomes only marginally significant if the single experiment with the largest effect is removed ($r = 0.41$, $P = 0.057$, $n = 22$). This weak correlation leaves open the possibility that LTF is caused by an increase in Ca^{2+} influx during action potentials. However, a weak correlation between two measures is also consistent with the possibility that the two measures reflect events that

are consequences of a third antecedent cause, but are themselves not causally related. With a view to testing this possibility, we attempted to better understand the origin of the increase in the presynaptic [Ca^{2+}]$_i$ signal.

Possible mechanisms underlying an increase in Ca^{2+} accumulation

Although Fig. 1 appears to implicate an increase in Ca^{2+} influx through voltage-dependent Ca^{2+} channels during LTF, other explanations of the results are possible. Presynaptic [Ca^{2+}]$_i$ depends on influx of Ca^{2+} ions, its uptake and removal by extrusion processes, and cytoplasmic Ca^{2+} buffering. A 1 min tetanus lasts long enough for [Ca^{2+}]$_i$ to reach a quasi-steady state plateau, and in principle an increase in that plateau could result from an increase in influx during the burst or a reduction in Ca^{2+} extrusion or uptake (Tank *et al.* 1995). An alteration in cytoplasmic Ca^{2+} buffering affects the kinetics of [Ca^{2+}]$_i$ changes in response to alterations in influx or efflux, but not steady-state levels. Moreover, an increase in Ca^{2+} influx could be through pathways other than voltage-dependent Ca^{2+} channels; Ca^{2+} entering via such routes might have no influence on transmitter release.

One way to distinguish among these possibilities is to look at the initial rate of rise in [Ca^{2+}]$_i$ during brief tetani, and its subsequent decay. An increase in Ca^{2+} influx through voltage-dependent channels might be associated with an increase in initial rate of rise, depending on how
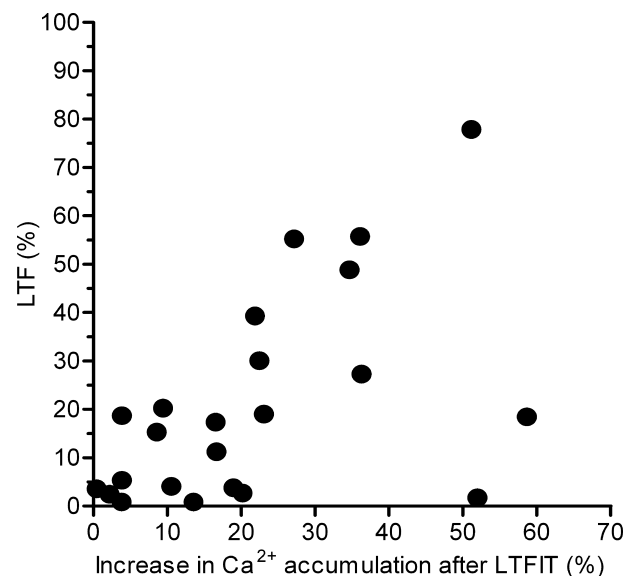
Figure 2. LTF and increased [Ca^{2+}]$_i$ are weakly correlated
The amount of LTF, expressed as percentage increase in 1 Hz EJPs following an LFT-inducing tetanus compared to those before the tetanus, is plotted versus the percentage increases in peak [Ca^{2+}]$_i$ following the LTF-inducing tetanus compared to those before the tetanus.

quickly it developed in a train, but there would be no change in the post-tetanic $[Ca^{2+}]_i$ decay rate. A reduced efflux or uptake mechanism would have little effect on the initial rate of $[Ca^{2+}]_i$ rise, since $[Ca^{2+}]_i$ only activates efflux and uptake as it increases and approaches its plateau. However, reduced efflux or uptake should be reflected in a reduction in post-tetanic $[Ca^{2+}]_i$ decay rate, which would also occur if there were an increase in cytoplasmic buffer power. From this it is clear that post-tetanic $[Ca^{2+}]_i$ decay is the most useful measure to discriminate changes in influx or efflux/uptake as responsible for an increased $[Ca^{2+}]_i$ plateau in a train.

We have looked for changes in both initial rate of $[Ca^{2+}]_i$ rise and post-tetanic $[Ca^{2+}]_i$ decay in bursts preceding and following an LTF-inducing tetanus. The data on initial rise are rather noisy, as they are subject to distortions from small muscle movements that often occur at the beginning of tetanic stimulation, and this measure is in any case not very diagnostic. Thus our measurements of changes in initial rate of $[Ca^{2+}]_i$ rise are inconclusive, and we will not present them. However, the decay of the $[Ca^{2+}]_i$ signal was often much smoother, and easily quantified since it was well fitted by a single exponential, and furthermore the results were consistent and statistically significant.

The post-burst decay in $[Ca^{2+}]_i$ is faster after an LTF-inducing tetanus

Figure 3*A* presents results from a typical experiment. In this preparation, $[Ca^{2+}]_i$ decayed more rapidly after test bursts following an LTF-inducing tetanus. This experiment was performed on 11 preparations. The decay of $[Ca^{2+}]_i$ was sometimes difficult to measure unambiguously during the PTP phase, when residual $[Ca^{2+}]_i$ was already declining. In most preparations, $[Ca^{2+}]_i$ decayed faster at this time. But in all 11 preparations, when $[Ca^{2+}]_i$ decay was measured after PTP had dissipated, it was faster after than before the LTF-inducing tetanus. This difference was statistically significant ($P < 0.001$, Fisher's sign test, 2-sided, Fig. 3*B*).
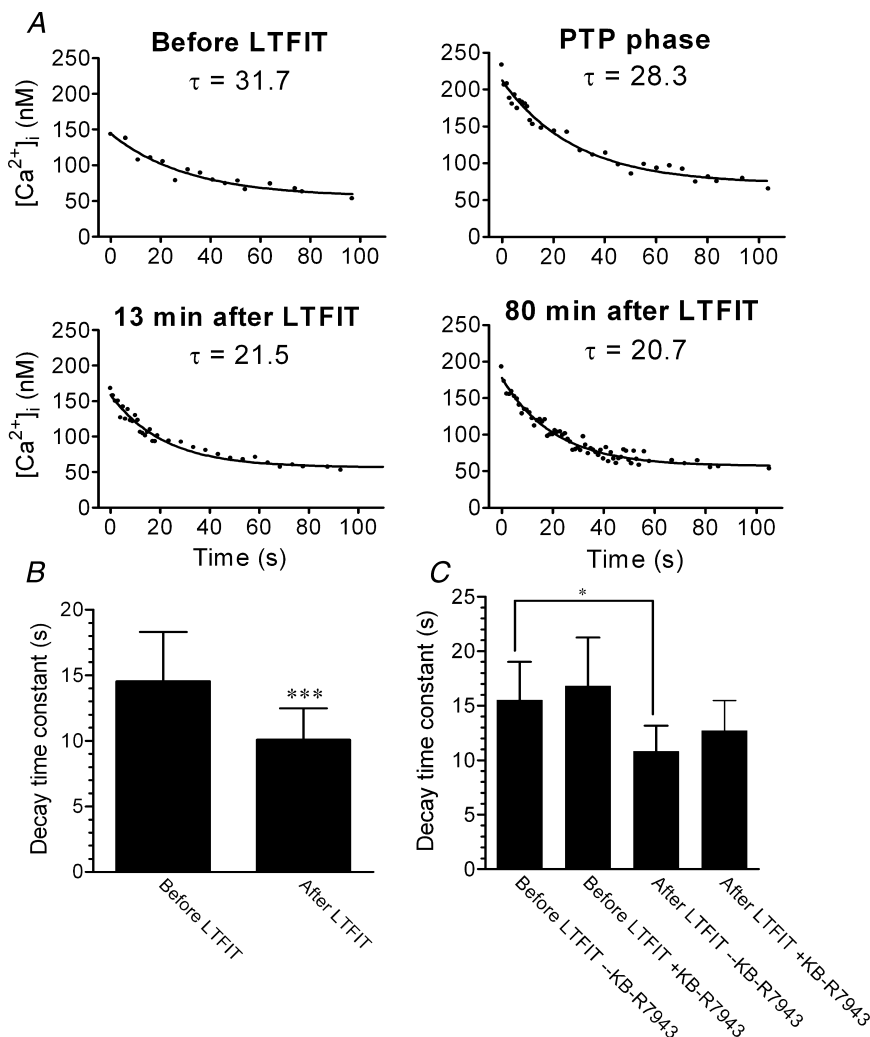
Figure 3. $[Ca^{2+}]_i$ decay kinetics are faster after the induction of LTF
The panels in *A* plot the $[Ca^{2+}]_i$ decay following a brief burst of motor neuron action potentials (10 Hz, 1 min) before an LTF-inducing tetanus (LTFIT), following an identical burst immediately after an LTF-inducing tetanus before PTP had dissipated, and 13 and 80 min after the end of the LTF-inducing tetanus when LTF was expressed in isolation. In *B*, $[Ca^{2+}]_i$ decay time constants after brief bursts before an LFTIT or at least 20 min afterwards were averaged from five preparations. Means and s.e.m. are plotted. *C* plots Ca^{2+} decay time constants before and after an LTF-inducing tetanus in the presence and absence of KB-R7943 (data of Fig. 4). *** and * denote significant differences ($P < 0.001$, $P < 0.05$, respectively).

From the reasoning outlined above, a faster $[Ca^{2+}]_i$ decay would follow from either a reduction in buffering, which would not affect steady-state $[Ca^{2+}]_i$ in a burst, or from an increase in Ca^{2+} efflux, which should lead to a *reduction* in steady-state $[Ca^{2+}]_i$ in a brief tetanus. Both of these scenarios contradict the results of Fig. 1. However, an alternative possibility presents itself. Na^+/Ca^{2+} exchange is one of the processes responsible for extruding cytoplasmic Ca^{2+} in these terminals (Mulkey & Zucker, 1992; Zhong *et al.* 2001). This process typically extrudes 1 Ca^{2+} ion in exchange for 3 Na^+ ions, and has a reversal potential that is normally just a little more positive than the resting potential. The Na^+/Ca^{2+} exchanger reverses during action potentials in a burst, admitting Ca^{2+} ions instead of extruding them. This could be a route by which additional Ca^{2+} ions accumulate in a test burst following an LTF-inducing tetanus. However, if the reversal potential for the exchanger remains above the membrane potential at the end of a brief tetanus, Ca^{2+} would then be extruded by this process (as well as by other pumps). Thus, an enhancement of Na^+/Ca^{2+} exchange following an LTF-inducing tetanus could be responsible for both the increased Ca^{2+} accumulation in short tetani and the more rapid decay of $[Ca^{2+}]_i$ afterwards.

The post-tetanic increase in [Ca^{2+}]$_i$ accumulation is due to Ca^{2+} influx through Na$^+$/Ca^{2+} exchange

In order to test for a role of Na^+/Ca^{2+} exchange in the increased $[Ca^{2+}]_i$ in bursts following an LTF-inducing tetanus, we made use of KB-R7943. Although initially thought of as an inhibitor of only reverse mode transport by the Na^+/Ca^{2+} exchanger, this drug actually blocks all transport of Na^+ and Ca^{2+} ions by this exchanger in either direction (Kimura *et al.* 1999; Elias *et al.* 2001), and is also a specific inhibitor of this process in invertebrates (Isaac *et al.* 2002). Our experimental protocol is illustrated in Fig. 4*A*. We compared simultaneously recorded EJPs and presynaptic $[Ca^{2+}]_i$ transients to 1 Hz stimulation interrupted by brief tetani (10 Hz for 1 min) before and after an LTF-inducing tetanus as in Fig. 1, with the additional feature that the preparation was exposed to 20 μM KB-R7943 for 11 min during one of the brief tetani before the LTF-inducing tetanus, and one afterwards. This drug had no effect on synaptic transmission at all, neither the 1 Hz baseline EJPs or transmission during brief tetani. There was also no effect on resting $[Ca^{2+}]_i$, nor on the accumulation of Ca^{2+} during a brief train before an LTF-inducing tetanus. Following this strong tetanus, transmission was enhanced for over 40 min, both at 1 Hz and in the 10 Hz trains, i.e. LTF was induced and expressed normally. Moreover, the increase in Ca^{2+} accumulation in brief tetani that usually accompanies LTF was observed in these experiments, but this increase was selectively blocked by KB-R7943, as was the increase in post-tetanic Ca^{2+} removal rate (Fig. 3*C*).

It has recently been reported (Santo-Domingo *et al.* 2007) that KB-R7943 also inhibits the mitochondrial Ca^{2+} uniporter, although with somewhat lower efficacy than inhibition of Na^+/Ca^{2+} exchange (Kimura *et al.* 1999). A post-tetanic increase in Ca^{2+} accumulation in test bursts could result from a reduction in uniporter Ca^{2+} uptake, but this would slow the Ca^{2+} removal rate at the end of a burst, the opposite of what we observed (Fig. 3). If KB-R7943 acted mainly to block mitochondrial uniporter transport, it would increase Ca^{2+} accumulation in test bursts, again contradicting our observations (Fig. 4). Our results are therefore inconsistent both with mitochondrial uniporter activity being the primary target of KB-R7943 and with uniporter modulation being responsible for the post-tetanic increase in Ca^{2+} accumulation in test bursts.

Dissociation of the increase in [Ca^{2+}]$_i$ in brief tetani from LTF of synaptic transmission

In 11 replications of this experiment, the average EJP amplitude at 1 Hz, measured during 2 min at least 20 min following an LTF-inducing tetanus, was significantly increased compared to the amplitudes just preceding an LTF-inducing tetanus ($P < 0.001$ by repeated measures ANOVA with Bonferroni's multiple comparison test). The Ca^{2+} accumulation in a 1 min burst 20 min following the LTF-inducing tetanus was also significantly increased compared to the accumulation measured 5 min before the strong tetanus ($P < 0.001$). KB-R7943 left LTF intact ($P < 0.01$), but blocked the increase in presynaptic Ca^{2+} accumulation during bursts ($P < 0.01$), so that there was no longer a difference in this measure in bursts preceding and following an LTF-inducing tetanus (Fig. 4*B*).

This dissociation of LTF from the increase in Ca^{2+} accumulation in a burst indicates that LTF cannot be a consequence of that increased accumulation, nor of the increase in Ca^{2+} influx through the Na^+/Ca^{2+} exchanger that underlies the increase in steady-state $[Ca^{2+}]_i$ in a train. Nevertheless, it appears that intense motor neuron activity modulates Na^+/Ca^{2+} function in some way, and we decided to investigate this further. Since addition of KB-R7943 affected neither resting $[Ca^{2+}]_i$ nor the Ca^{2+} accumulation in a burst preceding a strong tetanus in a rested neuron (Fig. 4*A*), this process normally contributes little to either the regulation of resting $[Ca^{2+}]_i$ or to the extrusion of Ca^{2+} ions entering in a brief tetanus. However, the effect of KB-R7943 on the $[Ca^{2+}]_i$ reached in a brief tetanus after a strong tetanus indicates that now Na^+/Ca^{2+} exchange is actively admitting Ca^{2+} ions during the burst and extruding them afterwards. This result

is consistent with our previous finding that Na^+/Ca^{2+} exchange plays an important role in regulating Ca^{2+} in strong tetani, admitting Ca^{2+} mainly in the latter part of a strong LTF-inducing tetanus and even for some time afterwards (Zhong *et al.* 2001). This suggests that strong tetani somehow activate the Na^+/Ca^{2+} exchanger, and that it remains more responsive in subsequent brief tetani.
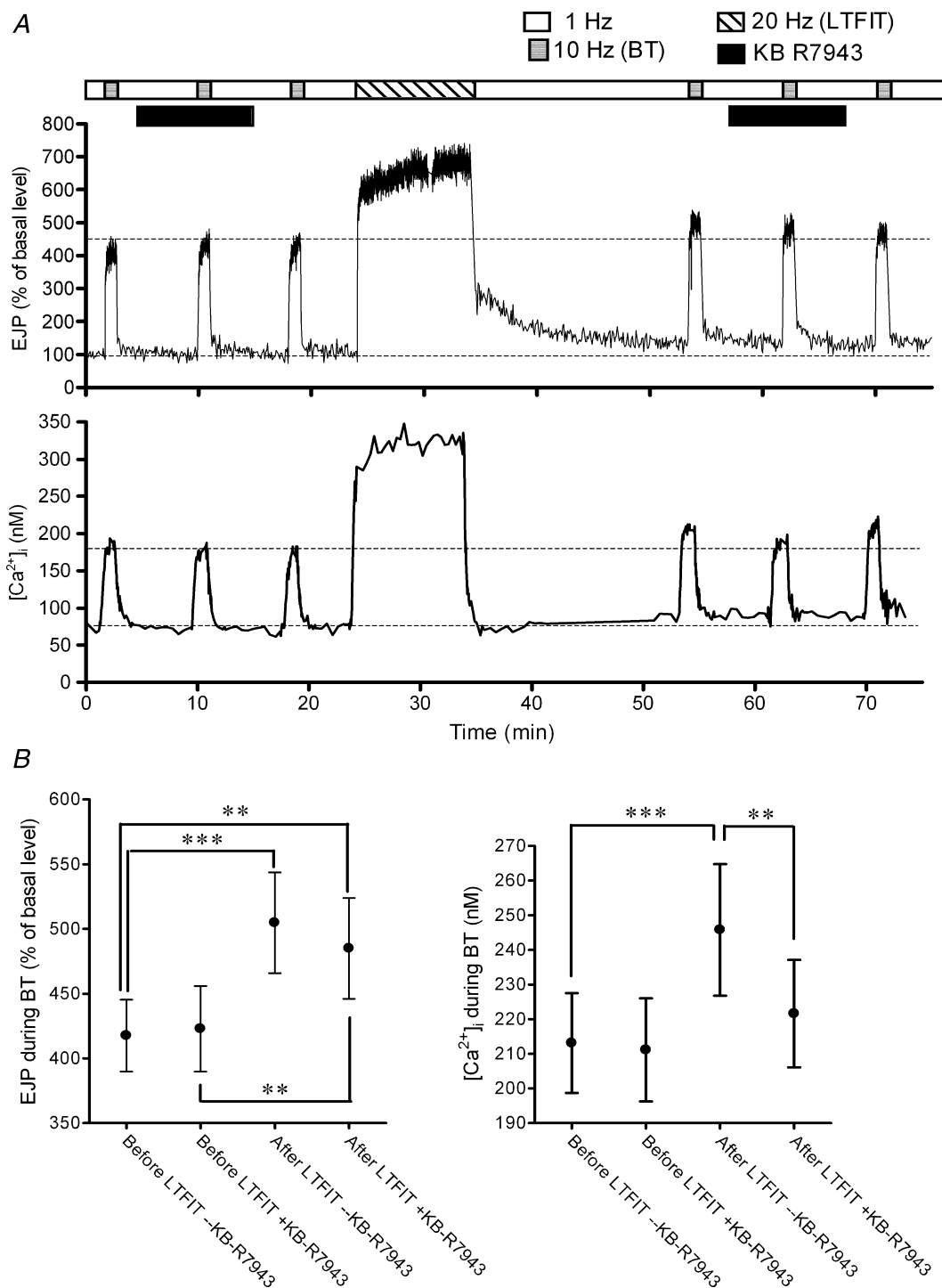
Figure 4. KB-R7943 (20 μM) blocks the increase in Ca^{2+} accumulation in brief tetani without affecting LTF

A, plots of normalized EJP amplitude and $[Ca^{2+}]_i$ as in Fig. 1*A*. *B* compares amplitudes of EJPs at the ends of brief bursts (left panel) and of plateau levels of $[Ca^{2+}]_i$ reached during those bursts (right panel) under four conditions: before and at least 20 min after an LTF-inducing tetanus, and in the presence or absence of KB-R7943. *** and ** denote significant differences ($P < 0.001$, $P < 0.01$, respectively).

The post-tetanic increase in Ca^{2+} influx is not an indirect consequence of modulation of Na$^+$/K$^+$-ATPase activity

Our results indicate that the post-tetanic increase in [Ca^{2+}]$_i$ accumulation is mediated by an alteration in the activity of Na$^+$/Ca^{2+} exchange. It has recently been found that [Ca^{2+}]$_i$ rapidly inhibits the activity of the Na$^+$/K$^+$-ATPase (Kim *et al.* 2007). Thus, it is possible that the increased post-tetanic Ca^{2+} influx could reduce the cell's ability to extrude Na$^+$. This would result in an elevated [Na$^+$]$_i$ accumulation in a post-tetanic burst, leading in turn to reversal of Na$^+$/Ca^{2+} exchange and amplification of the Ca^{2+} influx through this route. Alternatively, the heavy accumulation of Ca^{2+} ions in a strong tetanus could inhibit Na$^+$/K$^+$ transport in a subsequent burst, resulting in an increased accumulation of Na$^+$ and consequently an increase in Ca^{2+} influx through Na$^+$/Ca^{2+} exchange. The combination of short-term and long-term effects of elevated [Ca^{2+}]$_i$ on the Na$^+$/K$^+$-ATPase could thus conceivably be entirely responsible for the observed increase in Ca^{2+} influx through Na$^+$/Ca^{2+} exchange.

We tested this possibility by using the membrane hyperpolarization that develops during a burst as an assay of Na$^+$/K$^+$-ATPase activity. This hyperpolarization is completely blocked by ouabain in these motor nerve terminals (Wojtowicz & Atwood, 1988; Beaumont *et al.* 2002), so it is a sign of the activity of the Na$^+$/K$^+$-ATPase. To look for an immediate effect of Ca^{2+} influx in a burst on this pump, we compared the magnitudes of the hyperpolarization during 1 min bursts obtained in normal medium and in Ca^{2+}-free saline. If the [Ca^{2+}]$_i$ elevation during the burst inhibited Na$^+$/K$^+$ exchange, the tetanic hyperpolarization would have been reduced. Instead, the tetanic and post-tetanic hyperpolarizations were virtually identical under the two conditions (Fig. 5*A*). To test for a long-term effect of the large [Ca^{2+}]$_i$ elevation in a strong tetanus on subsequent Na$^+$/K$^+$-ATPase activity, we compared the hyperpolarization developing in pre- and post-tetanic bursts; these, too, were virtually identical (Fig. 5*B*). Because we found no evidence of a Ca^{2+}-dependent inhibition of Na$^+$/K$^+$ exchange, it appears very unlikely that such an effect is indirectly responsible for the post-tetanic enhancement of Na$^+$/Ca^{2+} activity.

Altered Na$^+$/Ca^{2+} exchange is not due to changes in membrane potential or ionic concentrations

The post-tetanic modulation of Na$^+$/Ca^{2+} exchange that we have demonstrated could arise in one of two ways: most simply, there could be a direct modification of exchange activity by recruiting dormant exchangers or modifying their function; alternatively, since the function of the Na$^+$/Ca^{2+} exchanger is sensitive to the membrane potential as well as internal and external Na$^+$ and Ca^{2+} activities, the increased Ca^{2+} influx could be due indirectly to a more depolarized average potential or a greater [Na$^+$] accumulation in the post-tetanic burst. To test the latter possibility, we have implemented a detailed
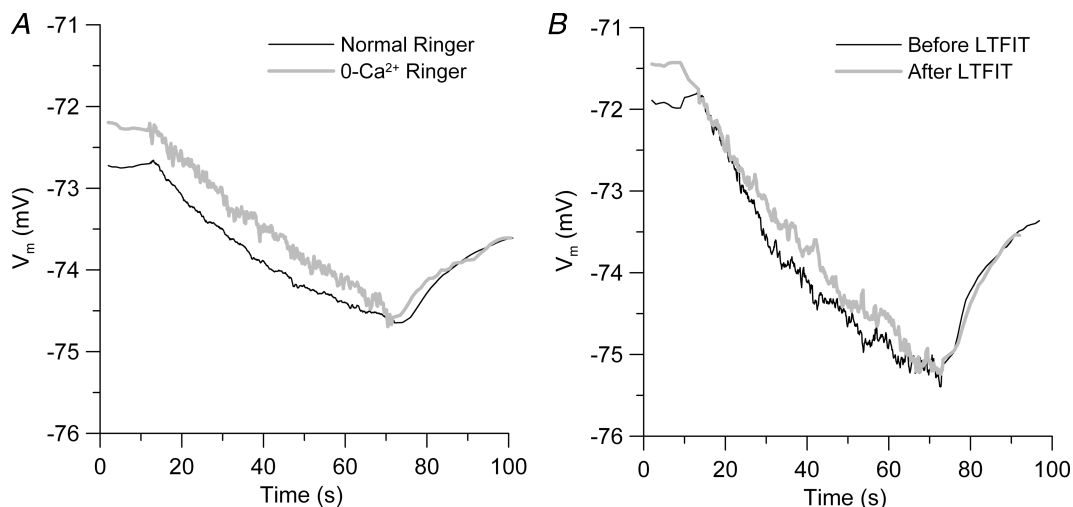
**Figure 5. Effect of Ca^{2+} influx on Na$^+$/K$^+$-ATPase activity**
A, stimulation of the motor neuron at 1 Hz was interrupted with a 1 min 10 Hz burst. The lines plot the hyperpolarization as the levels of membrane potential reached just before each action potential (with 5-point smoothing) in normal Ringer solution (black) and in 0-Ca^{2+} media (grey) on a finer voltage scale. *B*, the hyperpolarization accumulating in 1 min 10 Hz bursts 20 min before (black) and 45 min after (grey) a strong LTF-inducing tetanus are compared. Neither the Ca^{2+} entering in a 1 min burst nor the Ca^{2+} entering during a strong tetanus influenced the activity of Na$^+$/K$^+$-ATPase activity.

and well-tested kinetic model of the mammalian cardiac Na^+/Ca^{2+} exchanger (Kang & Hilgemann, 2004) in a BASIC program in order to predict ion transport through exchangers exposed to the recorded patterns of membrane potential, $[Na^+]_i$ and $[Ca^{2+}]_i$ profiles during pre- and post-tetanic bursts. We used the same parameters as in Kang & Hilgemann (2004), except that Na^+ and Ca^{2+} dissociation rates were each increased by 20% to account for the higher ionic strength of crayfish plasma and cytoplasm. For the purpose of these experiments we developed a new procedure to simultaneously measure $[Na^+]_i$ and $[Ca^{2+}]_i$ by measuring alternately the fluorescence of SBFI and fluo-4 from nerve terminals filled with both dyes.

Figure 6 shows presynaptic membrane potential and postsynaptic EJP amplitude (left panels) and $[Na^+]_i$ and $[Ca^{2+}]_i$ (right panels) measured before (Fig. 6A) and after (Fig. 6B) a strong tetanus that induced an LTF of 17%. The main difference between bursts before and after a strong tetanus is the larger $[Ca^{2+}]_i$ reached after the LTF-inducing tetanus. The measured time courses of presynaptic potential and ionic activities were used to drive the Kang–Hilgemann Na^+/Ca^{2+} exchanger model to produce the predictions illustrated in Fig. 7. The left panels show Na^+ and Ca^{2+} fluxes before (Fig. 7A) and after (Fig. 7B) tetanic stimulation. Initially, resting Na^+ influx drives Ca^{2+} efflux, and the fluxes reverse briefly during action potentials. During brief tetanic stimulation, as
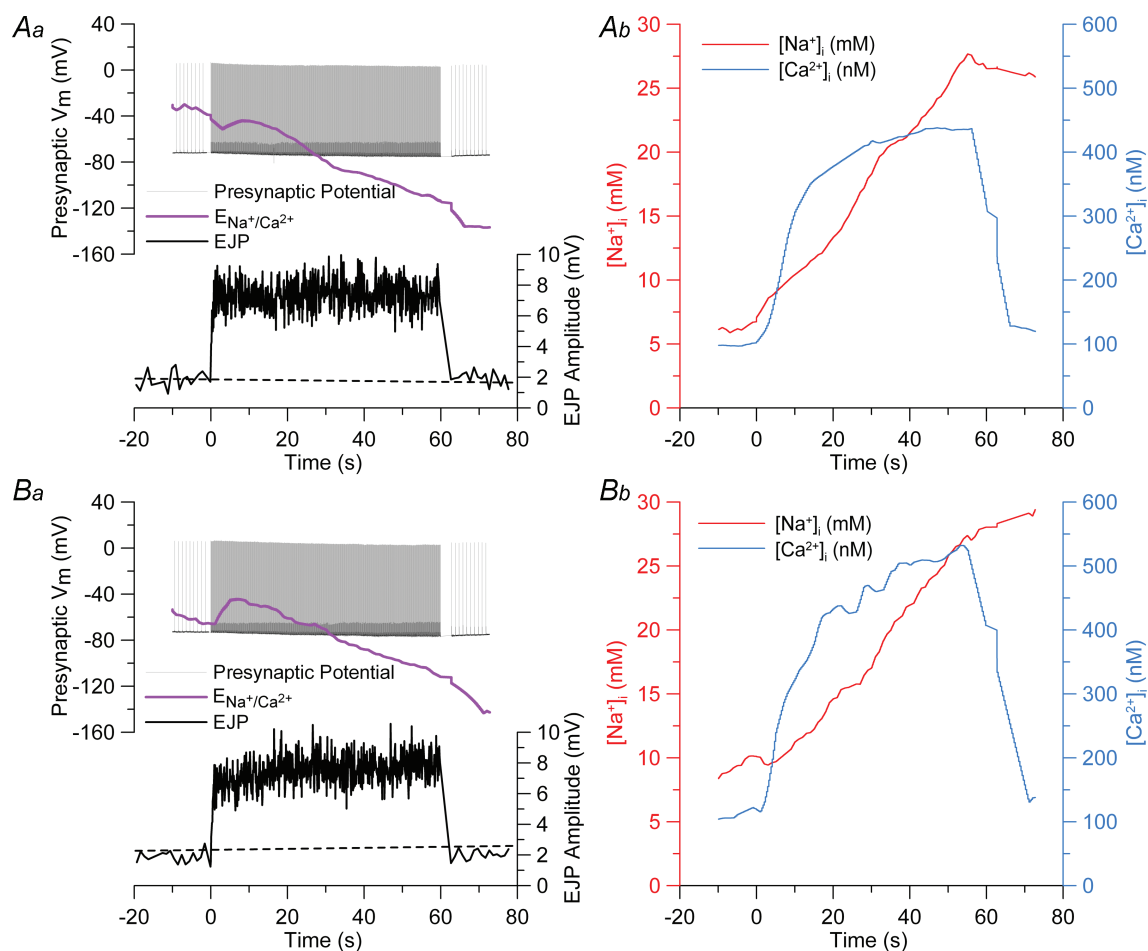

Figure 6. Simultaneous recording of pre- and postsynaptic potentials and presynaptic $[Na^+]_i$ and $[Ca^{2+}]_i$ before and after a strong tetanus

All measurements are for a brief action potential burst (10 Hz, from $t = 0$ to $t = 60$ s) before (*A*) or after (*B*) an LTF-inducing tetanus. *Aa* and *Ba* plot presynaptic membrane potential (upper traces, black) and calculated exchanger reversal potential ($E_{Na/Ca}$, violet) for the primary 3 Na^+ : 1 Ca^{2+} transport mode during a burst. *Ab* and *Bb* plot $[Na^+]_i$ (red) and $[Ca^{2+}]_i$ (blue) during a burst.

$[Na^+]_i$ accumulates, the transporter equilibrium potential (purple lines in Fig. 6) drops below the membrane potential, leading to Na^+ efflux and Ca^{2+} influx as transporters work in reverse mode. The right panels of Fig. 7 show the predicted accumulated flux of Ca^{2+} beginning at the start of a 1 min burst before (Fig. 7A) and after (Fig. 7B) strong tetanic stimulation. Ca^{2+} ions are

removed for the first 20 s of each burst (green zones), but by 35 s Ca^{2+} influx has matched the early efflux, and from then on (orange) Ca^{2+} ions accumulate intracellularly by virtue of reverse mode exchange. Thus the simulations predict our observed net influx of Ca^{2+} ions through Na^+/Ca^{2+} exchangers in a 1 min tetanus, resulting in an increase in $[Ca^{2+}]_i$ due to its operation. Remarkably, the simulations
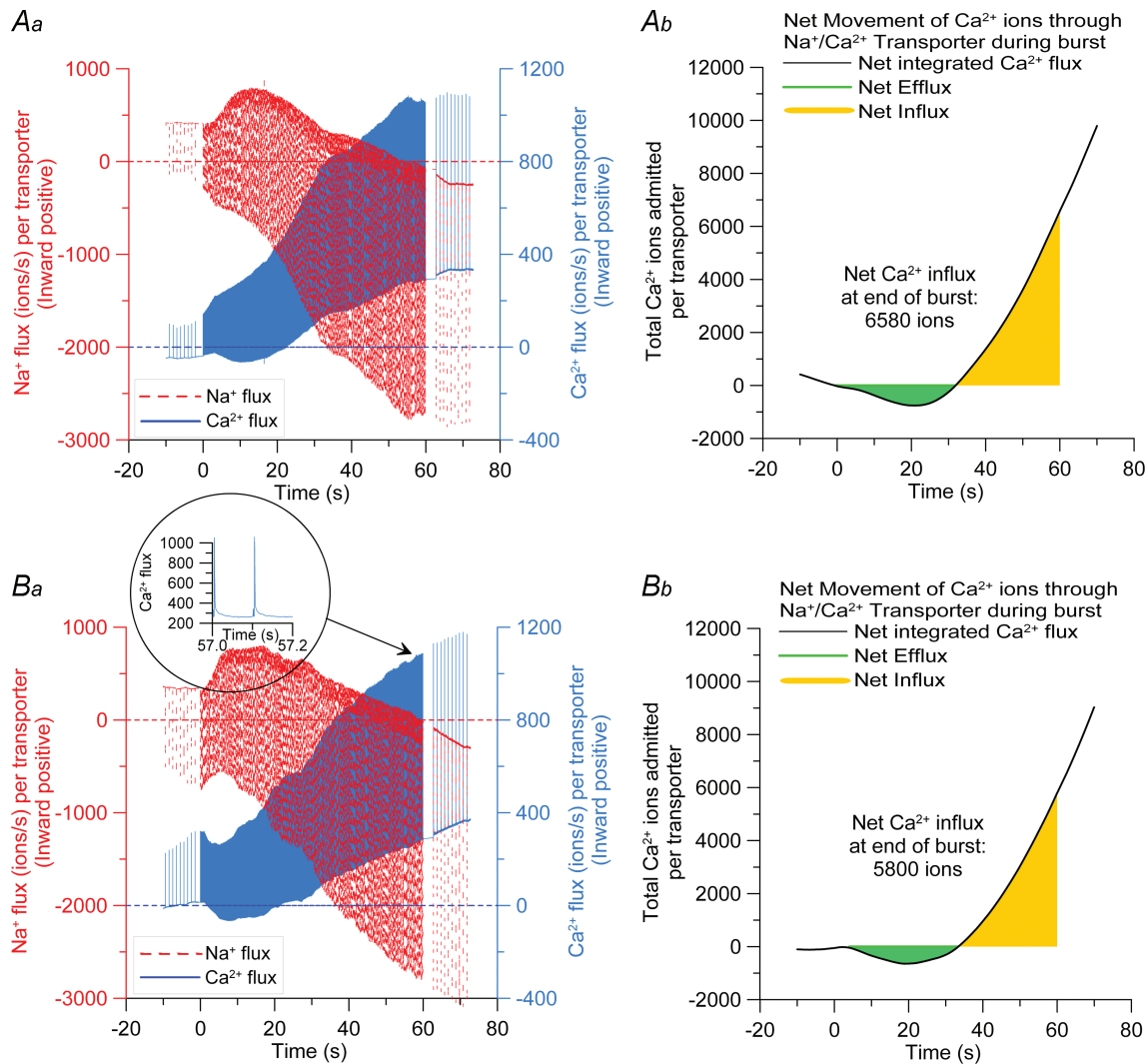
Figure 7. Calculated Na⁺ and Ca²⁺ fluxes and internal Ca²⁺ accumulation in bursts before and after a strong tetanus

Simulations showing the expected effects of changes in membrane potential, $[Na^+]_i$ and $[Ca^{2+}]_i$ after a strong tetanus on the accumulation of Ca^{2+} ions during test bursts. *Aa* and *Ba* show calculated Na^+ (red) and Ca^{2+} (blue) fluxes during a burst. The Na^+ fluxes are plotted as dashed red lines overlaid on Ca^{2+} fluxes plotted as continuous blue lines. Dotted lines show zero flux for Na^+ (red) and Ca^{2+} (blue). Ca^{2+} fluxes alternate between weak influx or efflux (at bottoms of blue regions) between action potentials and influx (at tops) during action potentials, as shown in inset in *Ba*, which is an expansion of the Ca^{2+} flux at the end of the burst. Shifts in Na^+ fluxes mirror those in Ca^{2+} fluxes as the membrane potential changes. *Ab* and *Bb* plot the calculated cytoplasmic accumulation of Ca^{2+} ions through one exchanger in a burst. During the first 20 s the net movement of Ca^{2+} is outward, resulting in a removal of Ca^{2+} ions. After 20 s this turns into a net inward movement, and Ca^{2+} ions begin to accumulate, leading to a net influx after about 30–35 s of stimulation. Therefore the reduction in $[Ca^{2+}]_i$ (green region) turns into a net increase in $[Ca^{2+}]_i$ (orange region) in the second half of the burst, of similar magnitude before and after an LTF-inducing tetanus.

indicate a nearly identical net Ca^{2+} accumulation before and after tetanic stimulation, actually slightly smaller (5800 ions per exchanger) after the strong tetanus than before it (6580 ions per exchanger). This behaviour was unaffected by small parameter changes in the model, and reflects the tendency of the transporter to more effectively remove Ca^{2+} ions in bursts with a larger measured Ca^{2+} accumulation.

Our measurements of pre- and post-tetanic Na^+ accumulation reveal them to be quite similar (see Figure 6*Ab* and *Bb*). This is a further test of the possibility that the heavy Ca^{2+} load imposed by a strong tetanus acted directly only to inhibit subsequent Na^+/K^+ exchange, leading to an increased Na^+ accumulation that in turn was exchanged for increased Ca^{2+} influx via reverse mode Na^+/Ca^{2+} exchange.

The conclusion to be drawn from these measurements and simulations is that the increased net influx of Ca^{2+} seen in a burst following a strong tetanus is not caused by differences in the membrane potential, $[Na^+]_i$, or $[Ca^{2+}]_i$ trajectories. Therefore, the observed post-tetanic increase in Ca^{2+} influx through Na^+/Ca^{2+} exchange must be due to a direct modulation of Na^+/Ca^{2+} transporter function. Either dormant transporters are activated, or the stoichiometric operation of the transporters is altered following intense activity.

Figure 7 makes another interesting prediction. Figure 7*Ab* and *Bb* predict that Ca^{2+} transport continues in an inward direction for some time after a 1 min burst, due to the persistent reduction in exchanger reversal potential (purple lines in Fig. 6). Thus, influx of Ca^{2+} through the Na^+/Ca^{2+} exchanger should counteract other Ca^{2+} extrusion and uptake processes, and an increase in Na^+/Ca^{2+} exchange activity should actually retard Ca^{2+} removal after a burst. This is exactly the opposite of our observation (Fig. 3) of a post-tetanic increase in Ca^{2+} removal rate. Figure 3*C* summarizes our measurements of Ca^{2+} removal time constants before and after a strong tetanus in the presence and absence of KB-R7943. Post-tetanic Ca^{2+} removal was faster, and this difference was diminished to insignificance by blocking Na^+/Ca^{2+} exchange with KB-R7943.

To understand why Ca^{2+} removal following a 1 min burst is faster after a strong tetanus at the same time that reverse mode Na^+/Ca^{2+} exchange is producing an extra Ca^{2+} influx, one must recognize that this process transports far less Ca^{2+} than other processes such as the Ca^{2+}-ATPase. In fact, before a strong tetanus, the role of Na^+/Ca^{2+} exchange is so small that the effect of its removal by KB-R7943 is undetectable. This, together with the rise of $[Ca^{2+}]_i$ to a quasi-steady level in less than 1 min in KB-R7943, indicates that remaining Ca^{2+} removal processes rise to equal the Ca^{2+} influx through voltage-dependent Ca^{2+} channels, and that these two balancing fluxes are much greater than Ca^{2+} movements

through Na^+/Ca^{2+} exchangers. Post-tetanic activation of Na^+/Ca^{2+} transport leads to an additional Ca^{2+} accumulation during a test burst. Since $[Ca^{2+}]_i$ reaches a higher steady-state level, there must be a corresponding increase in Ca^{2+} efflux to compensate for this, which occurs because $[Ca^{2+}]_i$ reaching a higher level activates more efflux. At these nerve terminals, Ca^{2+} is removed primarily by a plasma membrane Ca^{2+}-ATPase (Zhong *et al.* 2001) that depends nonlinearly on $[Ca^{2+}]_i$, with the removal rate constant increasing with higher $[Ca^{2+}]_i$ (Ohnuma *et al.* 1999). This property of the dominant Ca^{2+} removal process accounts for the increased rate of $[Ca^{2+}]_i$ decay following elevated Ca^{2+} accumulation in bursts following an LTF-inducing tetanus.

Possible biochemical mediators of Na^+/Ca^{2+} transport regulation

We imagine that electrical activity is coupled to regulation of Na^+/Ca^{2+} exchange by Ca^{2+}, acting perhaps through a kinase or phosphatase cascade to modulate transporters or other regulatory proteins. Cardiac and epithelial Na^+/Ca^{2+} transporters have been reported to be stimulated by protein kinase A- (PKA) and protein kinase C-dependent phosphorylation, respectively (Perchenet *et al.* 2000; Kita *et al.* 2004), while cardiac transport is inhibited by the Ca^{2+}-dependent phosphatase calcineurin (Katanosaka *et al.* 2005). We attempted to delineate biochemical pathways mediating regulation of Na^+/Ca^{2+} exchange by testing whether the increase in Ca^{2+} accumulation in a burst following an LTF-inducing tetanus was influenced by either a broad-spectrum protein kinase inhibitor or by an inhibitor of Ca^{2+}-dependent phosphatases. We used K-252a (1 μM), which inhibits both PKA and Ca^{2+}/calmodulin dependent kinase II, and cyclosporin (3 μM), which inhibits calcineurin. When applied for 20 min during the last of several test bursts and a subsequent LTF-inducing tetanus, neither drug had any effect on the Ca^{2+} accumulation in the pretetanic test burst nor on the subsequent enhancement of Ca^{2+} accumulation in test bursts. Another possibility is that increased Na^+/Ca^{2+} exchange activity might be a consequence of the well-known ATP dependence of this transporter (DiPolo & Beauge, 2006), especially if there is a rebound increase in presynaptic ATP levels following a strong tetanus. Discovery of the mediators of transport modulation will require further investigation.

Discussion

The chief findings of this study are: (1) an LTF-inducing tetanus causes an increase in the level of presynaptic $[Ca^{2+}]_i$ reached in a test (10 Hz, 1 min) burst of action potentials at crayfish leg opener motor nerve terminals,

which is mediated by an increased Ca^{2+} influx through Na$^+$/Ca^{2+} transporters operating in reverse mode, and (2) this increase in presynaptic [Ca^{2+}]$_i$ accompanying action potentials is not involved in the increase in transmitter release of LTF.

Our results have several implications

Just because action potentials appear to admit more Ca^{2+}, this does not necessarily imply that this increase in [Ca^{2+}]$_i$ must elicit more transmitter release. At crayfish NMJs, vesicle fusion is triggered by the localized rise in [Ca^{2+}]$_i$ in 'microdomains' arising from clusters of Ca^{2+} channels opening during an action potential (Zucker *et al.* 1991, 2003; Zucker, 1993). Na$^+$/Ca^{2+} exchangers are concentrated in nerve terminals, but are excluded from the active zone where vesicles are docked and Ca^{2+} channels are located (Luther *et al.* 1992; Juhaszova *et al.* 2000). Therefore, a modest influx through these transporters operating in reverse mode and leading to a rise in volume-average [Ca^{2+}]$_i$ of about 33 nm (Fig. 4) will have little effect on the peak [Ca^{2+}]$_i$ of about 20 μm reached in the microdomains where transmitter release is triggered (Ohnuma *et al.* 2001). This modest increase in [Ca^{2+}]$_i$ reached in a brief tetanus is also unlikely to influence the amounts of other forms of short-term plasticity occurring during the burst, such as facilitation, augmentation and post-tetanic potentiation (Delaney & Tank, 1994; Tang & Zucker, 1997), which explains why block of this increased Ca^{2+} accumulation in a burst has little effect on transmission during that burst (Fig. 4). Previous results showed that LTF induction requires a rise in presynaptic [Ca^{2+}]$_i$ during tetanic stimulation (Zhong & Zucker, 2004), and we presume that the activation of Na$^+$/Ca^{2+} transporters to admit Ca^{2+} during action potentials is also a consequence of the [Ca^{2+}]$_i$ rise during the strong tetanus. If enhanced Na$^+$/Ca^{2+} exchange activity and LTF are independent processes both activated by intracellular Ca^{2+}, this would lead to a correlation across preparations in the magnitudes of these responses to tetanic stimulation (Fig. 2).

If the correlation between magnitudes of LTF and increased [Ca^{2+}]$_i$ signal in a brief tetanus arises from their common dependence on the larger and more prolonged [Ca^{2+}]$_i$ accumulation in the LTF-inducing tetanus, then one might expect the former two variables to be correlated with the magnitude of the [Ca^{2+}]$_i$ rise during the strong tetanus. We tested for such correlations, and found them to be even weaker than the correlation between LTF and [Ca^{2+}]$_i$ accumulation through Na$^+$/Ca^{2+} exchange ($r = 0.19$–0.22 and $P = 0.3$–0.4; data not shown). A likely explanation for this is that both dependent variables (LTF magnitude and increase in Ca^{2+} influx through Na$^+$/Ca^{2+}

transport) are long lasting changes that are sensitive to past history. Specimens which have recently experienced intense motor neuron activity would already express LTF and activated Na$^+$/Ca^{2+} exchange at the beginning of an experiment, and should show smaller effects of further tetanization regardless of the level of [Ca^{2+}]$_i$ reached in a strong tetanus.

Our results reveal a previously unknown activity-dependent modulation of the activity of Na$^+$/Ca^{2+} transporters. Before an LTF-inducing tetanus, Ca^{2+} influx via Na$^+$/Ca^{2+} exchange during a 10 Hz, 1 min burst is a tiny fraction of total Ca^{2+} influx. The peak [Ca^{2+}]$_i$ in such a burst is not significantly reduced by KB-R7943 ($0.95 \pm 1.2\%$ reduction in the experiments of Fig. 4). However, after an LTF-inducing tetanus, the peak [Ca^{2+}]$_i$ accumulating in a brief burst increased by $15.2 \pm 3.9\%$, and this increase was blocked by KB-R7943. This suggests a substantial (probably many-fold) increase in Ca^{2+} influx through Na$^+$/Ca^{2+} exchange after a strong tetanus. Such an increase cannot be explained by effects of differences in the membrane potential, [Na$^+$]$_i$, or [Ca^{2+}]$_i$ profiles in bursts before and after intense activity, but instead appears to be due to a Ca^{2+}-dependent modulation of Na$^+$/Ca^{2+} transporters. We postulate that a large and prolonged rise in [Ca^{2+}]$_i$ occurring during sustained activity sensitizes this transporter, either by recruiting dormant transporters or by altering some aspect of their binding or transport of Na$^+$ or Ca^{2+} ions. This may allow cells to cope better with, and recover faster from, large Ca^{2+} loads.

It has recently been discovered that [Ca^{2+}]$_i$ can regulate a Cl$^-$ transporter (Woodin *et al.* 2003) and the plasma membrane Ca^{2+}-ATPase (Scheuss *et al.* 2006) in hippocampal neurons. Activity-dependent modulation of ion transport activity may be more widespread than hitherto expected.

Allana & Lin (2004) report the presence of Ca^{2+} influx through non-P, non-Q, non-N, non-L, non-R-type Ca^{2+} channels at crayfish opener inhibitor motor nerve terminals, which appear to be more distant from vesicles than the P-type Ca^{2+} channels evoking release. This component of Ca^{2+} influx did not normally support or modulate transmitter release, although it could do so under conditions of blockade of P-type Ca^{2+} channels and prolonged depolarization. It is possible that some, or even all, of this Ca^{2+} influx was mediated by reverse mode operation of the Na$^+$/Ca^{2+} transporter.

References

Allana TN & Lin JW (2004). Relative distribution of Ca^{2+} channels at the crayfish inhibitory neuromuscular junction. *J Neurophysiol* **92**, 1491–1500.

Atwood HL & Wojtowicz JM (1986). Short-term and long-term plasticity and physiological differentiation of crustacean motor synapses. *Int Rev Neurobiol* **28**, 275–362.

Beaumont V, Zhong N, Fletcher R, Froemke RC & Zucker RS (2001). Phosphorylation and local presynaptic protein synthesis in calcium- and calcineurin-dependent induction of crayfish long-term facilitation. *Neuron* **32**, 489–501.

Beaumont V, Zhong N, Froemke RC, Ball RW & Zucker RS (2002). Temporal synaptic tagging by I_h activation and actin: involvement in long-term facilitation and cAMP-induced synaptic enhancement. *Neuron* **33**, 601–613.

Beaumont V & Zucker RS (2000). Enhancement of synaptic transmission by cyclic AMP modulation of presynaptic I_h channels. *Nat Neurosci* **3**, 133–141.

Cheung U, Atwood HL & Zucker RS (2006). Presynaptic effectors contributing to cAMP-induced synaptic potentiation in *Drosophila*. *J Neurobiol* **66**, 273–280.

Delaney KR & Tank DW (1994). A quantitative measurement of the dependence of short-term synaptic enhancement on presynaptic residual calcium. *J Neurosci* **14**, 5885–5902.

Delaney K, Tank DW & Zucker RS (1991). Presynaptic calcium and serotonin-mediated enhancement of transmitter release at crayfish neuromuscular junction. *J Neurosci* **11**, 2631–2643.

DiPolo R & Beauge L (2006). Sodium/calcium exchanger: influence of metabolic regulation on ion carrier interactions. *Physiol Rev* **86**, 155–203.

Dudel J (1965). Facilitatory effects of 5-hydroxy-tryptamine on the crayfish neuromuscular junction. *Naunyn Schmiedebergs Arch Exp Pathol Pharmakol* **249**, 515–528.

Elias CL, Lukas A, Shurraw S, Scott J, Omelchenko A, Gross GJ, Hnatowich M & Hryshko LV (2001). Inhibition of Na^+/Ca^{2+} exchange by KB-R7943: transport mode selectivity and antiarrhythmic consequences. *Am J Physiol Heart Circ Physiol* **281**, H1334–H1345.

Fischer L & Florey E (1983). Modulation of synaptic transmission and excitation-contraction coupling in the opener muscle of the crayfish, *Astacus leptodactylus*, by 5-hydroxytryptamine and octopamine. *J Exp Biol* **102**, 187–198.

Glusman S & Kravitz EA (1982). The action of serotonin on excitatory nerve terminals in lobster nerve–muscle preparations. *J Physiol* **325**, 223–241.

Grynkiewicz G, Poenie M & Tsien RY (1985). A new generation of Ca^{2+} indicators with greatly improved fluorescence properties. *J Biol Chem* **260**, 3440–3450.

Habermann E (1989). Palytoxin acts through Na^+,K^+-ATPase. *Toxicon* **27**, 1171–1187.

Harootunian AT, Kao JP, Eckert BK & Tsien RY (1989). Fluorescence ratio imaging of cytosolic free Na^+ in individual fibroblasts and lymphocytes. *J Biol Chem* **264**, 19458–19467.

Isaac MR, Elias CL, Le HD, Omelchenko A, Hnatowich M & Hryshko LV (2002). Inhibition of the *Drosophila* Na^+/Ca^{++}) exchanger, CALX1.1, by KB-R7943. *Ann N Y Acad Sci* **976**, 543–545.

Juhaszova M, Church P, Blaustein MP & Stanley EF (2000). Location of calcium transporters at presynaptic terminals. *Eur J Neurosci* **12**, 839–846.

Kamiya H & Zucker RS (1994). Residual Ca^{2+} and short-term synaptic plasticity. *Nature* **371**, 603–606.

Kang TM & Hilgemann DW (2004). Multiple transport modes of the cardiac Na^+/Ca^{2+} exchanger. *Nature* **427**, 544–548.

Katanosaka Y, Iwata Y, Kobayashi Y, Shibasaki F, Wakabayashi S & Shigekawa M (2005). Calcineurin inhibits Na^+/Ca^{2+} exchange in phenylephrine-treated hypertrophic cardiomyocytes. *J Biol Chem* **280**, 5764–5772.

Kim JH, Sizov I, Dobretsov M & von Gersdorff H (2007). Presynaptic Ca^{2+} buffers control the strength of a fast post-tetanic hyperpolarization mediated by the $\alpha3$ Na^+/K^+-ATPase. *Nat Neurosci* **10**, 196–205.

Kimura J, Watano T, Kawahara M, Sakai E & Yatabe J (1999). Direction-independent block of bi-directional Na^+/Ca^{2+} exchange current by KB-R7943 in guinea-pig cardiac myocytes. *Br J Pharmacol* **128**, 969–974.

Kita S, Katsuragi T & Iwamoto T (2004). Endothelin-1 enhances the activity of Na^+/Ca^{2+} exchanger type 1 in renal epithelial cells. *J Cardiovasc Pharmacol* **44**, S239–S243.

Kuromi H & Kidokoro Y (2000). Tetanic stimulation recruits vesicles from reserve pool via a cAMP-mediated process in *Drosophila* synapses. *Neuron* **27**, 133–143.

Landò L & Zucker RS (1994). Ca^{2+} cooperativity in neurosecretion measured using photolabile Ca^{2+} chelators. *J Neurophysiol* **72**, 825–830.

Lau PM, Zucker RS & Bentley D (1999). Induction of filopodia by direct local elevation of intracellular calcium ion concentration. *J Cell Biol* **145**, 1265–1275.

Lin JW & Fu Q (2005). Modulation of available vesicles and release kinetics at the inhibitor of the crayfish neuromuscular junction. *Neuroscience* **130**, 889–895.

Luther PW, Yip RK, Bloch RJ, Ambesi A, Lindenmayer GE & Blaustein MP (1992). Presynaptic localization of sodium/calcium exchangers in neuromuscular preparations. *J Neurosci* **12**, 4898–4904.

Mulkey RM & Zucker RS (1992). Posttetanic potentiation at the crayfish neuromuscular junction is dependent on both intracellular calcium and sodium ion accumulation. *J Neurosci* **12**, 4327–4336.

Ohnuma K, Kazawa T, Ogawa S, Suzuki N, Miwa A & Kijima H (1999). Cooperative Ca^{2+} removal from presynaptic terminals of the spiny lobster neuromuscular junction. *Biophys J* **76**, 1819–1834.

Ohnuma K, Whim MD, Fetter RD, Kaczmarek LK & Zucker RS (2001). Presynaptic target of Ca^{2+} action on neuropeptide and acetylcholine release in *Aplysia californica*. *J Physiol* **535**, 647–662.

Perchenet L, Hinde AK, Patel KC, Hancox JC & Levi AJ (2000). Stimulation of Na/Ca exchange by the β-adrenergic/protein kinase A pathway in guinea-pig ventricular myocytes at 37°C. *Pflugers Arch* **439**, 822–828.

Santo-Domingo J, Vay L, Hernandez-Sanmiguel E, Lobaton CD, Moreno A, Montero M & Alvarez J (2007). The plasma membrane Na^+/Ca^{2+} exchange inhibitor KB-R7943 is also a potent inhibitor of the mitochondrial Ca^{2+} uniporter. *Br J Pharmacol* **151**, 647–654.

Scheuss V, Yasuda R, Sobczyk A & Svoboda K (2006). Nonlinear $[Ca^{2+}]$ signaling in dendrites and spines caused by activity-dependent depression of Ca^{2+} extrusion. *J Neurosci* **26**, 8183–8194.

Tang Y, Schlumpberger T, Kim T, Lueker M & Zucker RS (2000). Effects of mobile buffers on facilitation: experimental and computational studies. *Biophys J* **78**, 2735–2751.

Tang Y & Zucker RS (1997). Mitochondrial involvement in post-tetanic potentiation of synaptic transmission. *Neuron* **18**, 483–491.

Tank DW, Regehr WG & Delaney KR (1995). A quantitative analysis of presynaptic calcium dynamics that contribute to short-term enhancement. *J Neurosci* **15**, 7940–7952.

Wang C & Zucker RS (1998). Regulation of synaptic vesicle recycling by calcium and serotonin. *Neuron* **21**, 155–167.

Wojtowicz JM & Atwood HL (1985). Correlation of presynaptic and postsynaptic events during establishment of long-term facilitation at crayfish neuromuscular junction. *J Neurophysiol* **54**, 220–230.

Wojtowicz JM & Atwood HL (1986). Long-term facilitation alters transmitter releasing properties at the crayfish neuromuscular junction. *J Neurophysiol* **55**, 484–498.

Wojtowicz JM & Atwood HL (1988). Presynaptic long-term facilitation at the crayfish neuromuscular junction: voltage-dependent and ion-dependent phases. *J Neurosci* **8**, 4667–4674.

Wojtowicz JM, Marin L & Atwood HL (1994). Activity-induced changes in synaptic release sites at the crayfish neuromuscular junction. *J Neurosci* **14**, 3688–3703.

Wojtowicz JM, Parnas I, Parnas H & Atwood HL (1988). Long-term facilitation of synaptic transmission demonstrated with macro-patch recording at the crayfish neuromuscular junction. *Neurosci Lett* **90**, 152–158.

Woodin MA, Ganguly K & Poo MM (2003). Coincident pre- and postsynaptic activity modifies GABAergic synapses by postsynaptic changes in Cl$^-$ transporter activity. *Neuron* **39**, 807–820.

Wright SN, Brodwick MS & Bittner GD (1996). Presynaptic calcium currents at voltage-clamped excitor and inhibitor nerve terminals of crayfish. *J Physiol* **496**, 347–361.

Xia Y & Zucker RS(2005). Increase in Ca^{2+} influx in long-term facilitation at crayfish neuromuscular junctions. *2005 Abstract Viewer/Itinerary Planner 733.18.* Society for Neuroscience, Washington, DC.

Yoshihara M, Suzuki K & Kidokoro Y (2000). Two independent pathways mediated by cAMP and protein kinase A enhance spontaneous transmitter release at *Drosophila* neuromuscular junctions. *J Neurosci* **20**, 8315–8322.

Yoshihara M, Ueda A, Zhang D, Deitcher DL, Schwarz TL & Kidokoro Y (1999). Selective effects of neuronal-synaptobrevin mutations on transmitter release evoked by sustained versus transient Ca^{2+} increases and by cAMP. *J Neurosci* **19**, 2432–2441.

Zhong N, Beaumont V & Zucker RS (2001). Roles for mitochondrial and reverse mode Na$^+$/Ca^{2+} exchange and the plasmalemma Ca^{2+} ATPase in post-tetanic potentiation at crayfish neuromuscular junctions. *J Neurosci* **21**, 9598–9607.

Zhong N, Beaumont V & Zucker RS (2004). Calcium influx through HCN channels does not contribute to cAMP-enhanced transmission. *J Neurophysiol* **92**, 644–647.

Zhong N & Zucker RS (2004). Roles of Ca^{2+}, hyperpolarization and cyclic nucleotide-activated channel activation, and actin in temporal synaptic tagging. *J Neurosci* **24**, 4205–4212.

Zhong N & Zucker RS (2005). cAMP acts on exchange protein activated by cAMP/cAMP-regulated guanine nucleotide exchange protein to regulate transmitter release at the crayfish neuromuscular junction. *J Neurosci* **25**, 208–214.

Zucker RS (1993). Calcium and transmitter release. *J Physiol Paris* **87**, 25–36.

Zucker RS, Delaney KR, Mulkey R & Tank DW (1991). Presynaptic calcium in transmitter release and posttetanic potentiation. *Ann N Y Acad Sci* **635**, 191–207.

Zucker RS, Kullman DM & Schwarz TL (2003). Release of neurotransmitters. In *Fundamental Neuroscience*, 2nd edn, ed.Squire LR, Bloom FE, McConnell SK, Roberts JL, Spitzer NC & Zigmond MJ, pp. 155–192. Academic Press, San Diego.

Acknowledgements